Sirte University Scientific Journal (SUSJ)

Journal home page: http://journal.su.edu.ly/index.php/SUSJ/index

DOI: 10.37375/susj.v13i2.2500

Experimental Comparison Between Conductive and Capacitance Wire-Mesh Sensors to Predict Gas Void Fraction and Flow Regimes in Vertical Pipes

Almabrok Abushanaf Almabrok

Petroleum Engineering Department, Faculty of Engineering, Sirte University, Sirte, Libya.

DOI: 10.37375/susj.v13i2.2500

ARTICLE INFO:

Received 13 September 2023.
Accepted 19 November 2023.
Available online 01 December 2023.

Keywords: (*CondWMS, CapWMS, Void Fraction, Flow Regimes, Time Traces, PDF*)

A B S T R A C T

A comparative study of conductive and capacitance wire-mesh sensors was carried out for a wide range of gas velocities and for a fixed liquid velocity of 1.5 m/s. The two instruments were mounted on the vertical pipe at the highest and lowest positions of the downward and upward orientations in order to predict the gas void fraction and establish various flow regimes. The principle of conductive WMS is based on the discrepancies between the conductivity of the gas and liquid, while the principle of capacitance WMS is based on the variation of the permittivity between the two-phase. During the run of the experiments, the frequency was set at 1,000 Hz for one minute.

Averaged time traces of gas void fraction and its probability density function (PDF) and distributions of gas void fraction were applied to confirm the similarities or discrepancies between the two techniques. It was observed that the gas void fractions obtained by both techniques displayed similar behavior. Although conductive WMS exhibited higher void fraction values than those measured by capacitance WMS.

The cross-sectional and sliced images (i.e., reconstructed images) were also extracted from conductive and capacitance wire-mesh sensors at higher and lower locations of the upward section, which were used as another means to confirm the above-mentioned results. It was noted from the images that both devices depicted similar flow patterns for each particular flow rate.

1 Introduction

Liquid-gas two-phase flow plays a significant role in many engineering applications, such as in the production facilities of petroleum, heat transfer equipment, and boilers (A. Mešić et al. (2020)). The two-phase flow has different characteristics depending on the pipe orientation, pipe diameter, and flow conditions (L. A. Abdulkareem et al. 2016). Many researchers have investigated the two-phase flow phenomenon using empirical models and experimental work. Wire mesh sensors (WMS), electrical capacitance tomography (ECT), X-ray tomography, and ultrasound are widely used for measuring the gas void fraction in order to identify the flow regimes (U. Hampel et al., 2005;Y. Murai et al., 2009; M. G. Rasteiro et al., 2011; Mahmood et al., 2019). L. A. Abdulkareem et al. (2010) and V.A. Musa et al. (2021) reported the results of flow regimes by measuring the gas void fraction in horizontal pipes. They observed the flow regimes and classified their types based on the averaged time traces of the void fraction. Jones and Zuber (1975) also reported experimental data on flow regimes in vertical rectangular pipes using the X-ray technique. Their results were based on an analysis of the averaged gas void fraction. V. A. Musa et al. (2021) also used WMS as another means to collect data on the spatial distribution of two-phase flow in a vertical direction. L. A. Abdulkareem et al. (2021) identified the liquid holdup using PDF and PSD methods to determine the flow types in vertical and inclined pipes, respectively. Xie et al. (1989) used ECT tomography as a non-intrusive technique to observe the phase distribution in a dielectric pipe. They noted that the cost of the ECT device is lower than the other techniques and can give reliable images with high-speed captions. Almabrok et al. (2016) and Aliyu et al. (2017) installed capacitance WMS at different positions of serpentine pipes (i.d., 101.6 mm) to investigate the flow regimes in downward and upward directions, respectively. They observed different flow regimes using reconstructed images extracted by WMS and confirmed their results by employing the PDF of the averaged gas void fraction. Ali et al. (2021) carried out experimental work to investigate liquid-gas two-phase flow in inclined pipes with orientations of 45, 60, and 80 degrees using wire mesh sensors (WMS) and electrical capacitance tomography (ECT). They reported data on the cross-sectional void fraction of the gas-oil in the form of time traces and the probability density function (PDF) of the gas void fraction.

2 Description of the test facility

The experimental apparatus shown in Figure 1 was designed to attain the required data. The liquid is pumped from the storage tank by a special variable pump through the 180-degree bend, and the gas is supplied by the Delta V system through a T-shaped valve installed at the middle position of the upward section. The test facility comprises three vertical pipes connected together by three bends. The wire mesh sensors were structured at different locations throughout the facility in order to perform the purpose of this study.

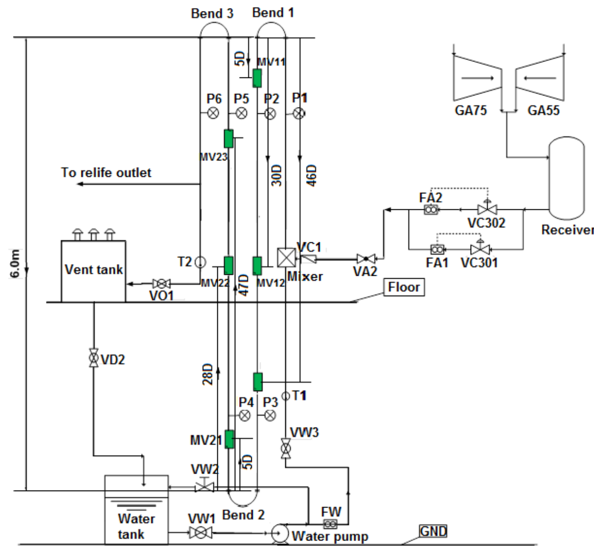

Figure 1: full description of the test facility

3 Basic principles of wire-mesh sensors

Conductive and capacitance wire mesh sensors are intrusive devices used locally to visualize the fluid behavior in the cross-sectional area of the flow line. These techniques have a high spatial resolution and are designed to give reliable imaging of the mixture and allow detailed estimation of the gas void fraction, as presented in Figure 2a. Both WMSs are operated at 1000 frames per second and have a 32×32 wire grid with an internal diameter of 101.6 mm. They comprise two perpendicular planes spaced by 2 mm. The measurements of the void fraction are based on transmitter and receiver wires (Figure 2b). The void fraction measurement of the condWMS depends on the measurement of the local conductivity of the tested fluids, while the measurement of the capWMS is based on the permittivity of the mixture. The data for the void fraction can be obtained by converting the measured raw data.

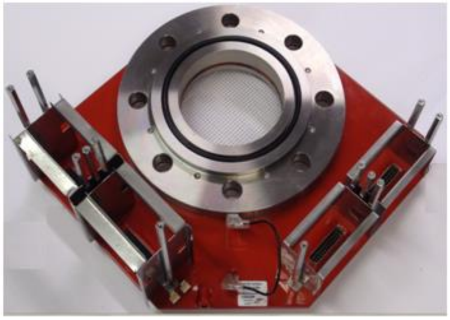

(a)

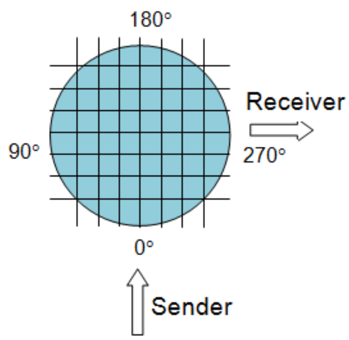

(b)

Figure 2: (a) wire-mesh sensor and (b) the two sets of wire electrodes

4 Results of experimental work

4.1 Variations of void fraction against gas superficial velocities

Figure 3 (a and b) presents the behavior of the gas phase for liquid velocity = 1.5 m/s and for a wide range of gas velocities. The results illustrated in Figure 3 were extracted from conductive and capacitance wire-mish sensors. The two devices are installed at the higher and lower sections of the vertical upward and downward pipes. It can be clearly noted from Figure 3 that both techniques presented similar characteristics of the gas void fraction, where the void fraction of the gas phase increased systematically with increasing gas velocities.

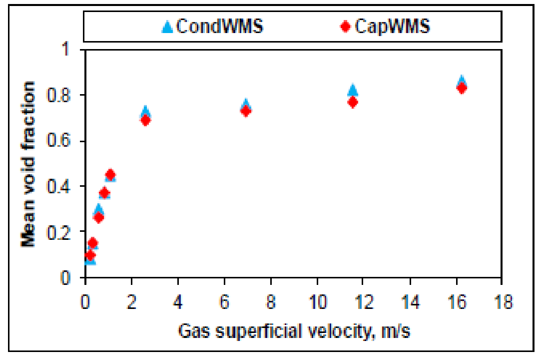

(a)

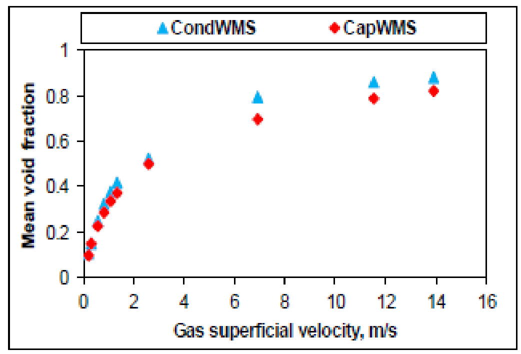

(b)

Figure 3: behavior of the void fraction against gas velocities at (a) the lower downward section and (b) the higher upward section

4.2 Comparison of void fraction measured by condWMS and capWMS

The plots illustrated in Figure 4 (a) and (b) show a linear deviation with very close values of gas void fraction for the two techniques. A negligible discrepancy was noted between CondWMS and Cap WMS at the higher location of upward orientation. This was due to the different timing of the measurement's executions. The uncertainty was estimated between 0 and 9.81% for the higher location of the upward orientation and -1.66 and 5.32% for the lower location of the downward orientation. It can be concluded from the plots that for the same flow rates, the Cond and Cap wire mesh sensors detected the same flow regime, which was a bubbly flow. Although the difference in the results varied to some degree for the other flow regimes.

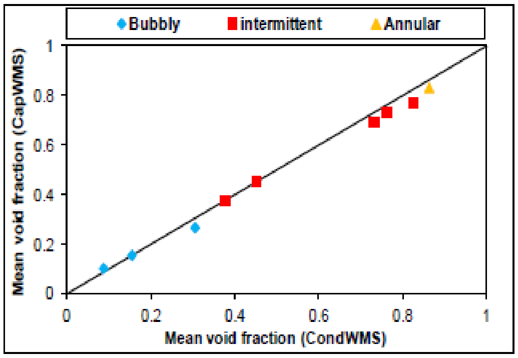

(a)

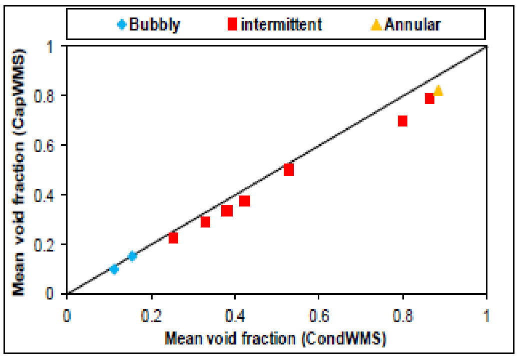

(b)

Figure 4: shows the void fraction and the flow regimes extracted from the CondWMS and CapWMS at (a) the lower downward section and (b) the higher upward section

4.3 Void fraction distribution identified by condWMS and capWMS

Time traces of the gas void fraction and the PDF are applied to clarify the flow characteristics inside the vertical pipe.

Figures 5 and 6 illustrate the experimental results generated by conductive and capacitance wire mesh sensors at the higher and lower locations of the downward and upward orientations, respectively. The gas void fraction depicted by the two techniques was almost identical when the same conditions were applied. This evidence of similarity is also noted in PDF data; however, a slightly higher amplitude can be noted in the results of CapWMS. This discrepancy was only observed at low gas flow rates (namely for gas velocities of 0.18, 0.54, and 2.56 m/s) in the region of bubbly and intermittent flow regimes. It was also noted at the transition region from intermittent to annular flows (i.e., for a gas velocity of 11.52 m/s) that the results of CondWMS depicted higher values of PDFs. Moreover, the gas void fraction extracted by the CondWMS was higher at the pipe wall than that extracted by the CapWMS. This may be due to the fact that the conductive wire mesh sensor is unable to accurately measure the flow near the pipe wall. The PDF's shape and the values of the corresponding gas void fraction at the lower and higher locations of the upward and downward orientations were identical for the high and low gas velocities.

CondWMS and CapWMS were also used to depict the local distributions of gas void fraction in downward and upward sections of the vertical pipeline, as shown in Figures 5 and 6, respectively. The results were obtained locally from 0^{o} to 180^{o} and from 90^{o} to 270^{o} for each technique. The experiments were carried out for different gas flow conditions and a fixed liquid flow rate. The principle of this work was based on measuring and averaging the gas void fraction that was obtained at each particular wire, which ranged from 15 to 18. Both devices presented similar behavior in terms of gas void fraction when high gas flow rates were applied. These results confirm the previous measurements (i.e., time traces and PDF) of the void fraction conducted by CondWMS and CapWMS. The data obtained at the upward orientation presented similar shapes of averaged time traces, PDFs, and local distributions of gas void fraction. The discrepancy between the two techniques was observed at the pipe wall for downward orientation. It was noted that CapWMS provided low values of local void fraction distribution when the flow reached the pipe wall, while CondWMS gave higher void fraction values close to the pipe wall. It can be confirmed that the CapWMS provides accurate information on the gas phase fraction at the inner pipe wall. This is due to the fact that most of the gas phase is always distributed in the pipe core and the liquid phase is concentrated on the pipe wall. The wall peak of the void fraction was obviously observed by CondWMS measurements. This means that the CondWMS presented less information about gas distribution close to the pipe wall.

4.4 Flow behavior depicted by condWMS and capWMS

Reconstructed images of cross-sectional area and corresponding sliced images were also depicted by both instruments to illustrate the flow types that formed during the measurements, as presented in Figure 7. These measurements reflect the flow behavior inside the vertical pipeline and give a clear picture of the generated flow regimes.

Figure 7 illustrates the cross-sectional area of the gas void fraction in the form of sliced images identified by CondWMS and CapWMS at the higher location of the upward section. These results were obtained at a wide range of gas velocities and a constant liquid velocity of 1.5 m/s. The blue color indicates the liquid phase, while the red color indicates the gas phase. It was noted that both techniques presented an identical flow pattern at each particular gas flow rate.

The bubbly flow regime was identified by conductive and capacitance WMS for relatively low flow rates. This flow type was characterized by uniformly small bubbles accompanied by larger ones. The bubbles were uniformly distributed and occupied the pipe center. The large bubbles were spherical, and their sizes were notably smaller than the pipe center. Increasing the gas flow rate leads to the coalescence of these bubbles, and a transition region takes place as a result. An intermittent flow regime was formed due to the further increase in gas flow rates. Eventually, annular flow was generated as the gas flow rates increased to higher values. This flow type is characterized by a liquid film on both sides of the pipe and a gas phase in the center. It was observed in this flow region that the gas phase was accompanied by a huge number of droplets.

5 Conclusion

In this study, a comparison between conductive (Cond) and capacitance (Cap) wire mesh sensors was successfully achieved using liquid-gas two-phase flow in vertical pipes with a serpentine configuration. Time series, probability density function (PDF), and local gas void fraction are used to reveal the difference or similarity between the CondWMS and CapWMS. The analyzed data were confirmed using reconstructed images that were extracted from both sensors. The results of the current study are summarized as follows:

1. The comparison between CondWMS and CapWMS was performed, and the results were similar. However, there was a negligible difference at some flow rates.
2. For the same flow conditions, the estimated flow regimes identified by the CondWMS agreed with those identified by the CapWMS.
3. At a constant liquid velocity and for a wide range of gas velocities, both sensors show a steep increase in gas void fraction close to the pipe center. This behavior was in contrast to the pipe wall.
4. Bubbly, intermittent, and annular flows were observed by the two sensors for the same range of flow rates.
5. The gas and liquid flow rates had a significant impact on the flow regimes.
6. Both techniques accurately measured and depicted the gas-liquid void fraction in large vertical pipes.

References

Ali I. Hameed, Lokman A. Abdulkareem, and Raid A. Mahmood (2021). Experimental Comparison Between Wire Mesh and Electrical Capacitance Tomography Sensors to Predict a Two-Phase Flow Behaviour and Patterns in Inclined Pipe. Technium vol. 3, Issue 5, pp.49-63 (2021) ISSN: 2668–778X.

Aliyu M. Aliyu, Almabrok A. Almabrok, Yahaya D. Baba, Liyun Lao, Hoi Yeung, and Kyung Chun Kim (2017). Upward Gas–Liquid Two-Phase Flow After a U-bend in a Large-Diameter Serpentine Pipe. International Journal of Heat and Mass Transfer, vol.108, pages 784–800.

Almabrok A. Almabrok, Aliyu M. Aliyu, Liyun Lao, and Hoi Yeung (2016).Gas/Liquid Flow Behaviours in a Downward Section of Large Diameter Vertical Serpentine Pipes. International Journal of Multiphase Flow, vol. 78, 2016, pages 25–43.

A. Mešić, I. Delić, and N. Ganibegović (2020). Numerical modeling of multiphase flow inside the aero mixture channel and low-emission burner of boiler OB-650. Technium: Romanian Journal of Applied Sciences and Technology, vol. 2, no. 7, pp. 94–106.

L. A. Abdulkareem, E. Escrig, B. N. Reinecke, S. Hewakandamby, and B. J. Azzopardi (2016). Tomographic interrogation of gas-liquid flows in inclined risers. ICMF – 9th International Conference on Multiphase Flow.

L. A. Abdulkareem, S. Sharaf, B. J. Azzopardi, and A. Hunt (2010). Effect of Inclination on Slug Flow Characteristics. Proceedings of the ASME 2010 International Mechanical Engineering Congress & Exposition, pp. 735–742.

L. A. Abdulkareem, V. A. Musa, R. A. Mahmood, and E. A. Hasso (2021). Experimental Investigation of Two-Phase Flow Patterns in a Vertical to Horizontal Bend Pipe Using Wire-Mesh Sensor. Revista de Chimie, vol. 71, no. 12, pp. 18–33.

Jones, Jr. O. C. and Zuber, N. (1975). The Interrelation between Void Fraction Fluctuations and Flow Pattern in Two-Phase Flow. International Journal of Multiphase Flow, vol. 2, pp. 273–306.

M. G. Rasteiro, R. Silva, F. A. P. Garcia, and P. Faia (2011). Electrical tomography: a review of configurations and applications to particulate processes. KONA Powder Part. J., vol. 29, no. 29, pp. 67–80.

Mahmood, R.A., D. Buttsworth, and R. Malpress (2019). Experimental and Numerical Investigation of Two-phase Flow Orientation Direction Change on a Vertical Flash Tank Separator. International Journal of Management and Applied Science (IJMAS). 5 (4): p. 25–29.

Mahmood, R., D. Buttsworth, and R. Malpress (2019). Computational and Experimental Investigation of using an Extractor in the Vertical Gravitational Flash Tank Separator. International Journal of Automotive and Mechanical Engineering. 16 (2): p. 6706–672.

Mahmood, R.A., D. Buttsworth, and R. Malpress (2019). Computational and Experimental Investigation of the Vertical Flash Tank Separator Part 1: Effect of Parameters on Separation Efficiency. International Journal of Air-Conditioning and Refrigeration.

U. Hampel, M. Speck, H. J. Menz, D. Hoppe, E. Schleicher, and H. M. Prasser (2005). Experimental ultra fast x-ray computed tomography with a linearly scanned electron beam source. Flow Meas. Instrum., vol. 16, no. 2–3, pp. 65–72.

V. A. Musa, R. A. Mahmood, S. M. N. Khalifa, O. M. Ali, and L. A. Abdulkareem (2021). Flow Patterns of Oil-Gas and Pressure Gradients in Near-Horizontal Flow Pipeline : Experimental Investigation Using Differential Pressure Transducers, vol. 39, no. 2, pp. 621–628.

Xie, C.G., Plaskowski, A., Beck, and M.S. (1989). 8-Electrode Capacitance System for Two-component Flow Identification. IEE proceeding Pt. A, 136, pp. 184–190.

Y. Murai, S. Ohta, A. Shigetomi, Y. Tasaka, and Y. Takeda (2009). Development of an ultrasonic void fraction profiler. Meas. Sci. Technol., vol. 20, no. 11.

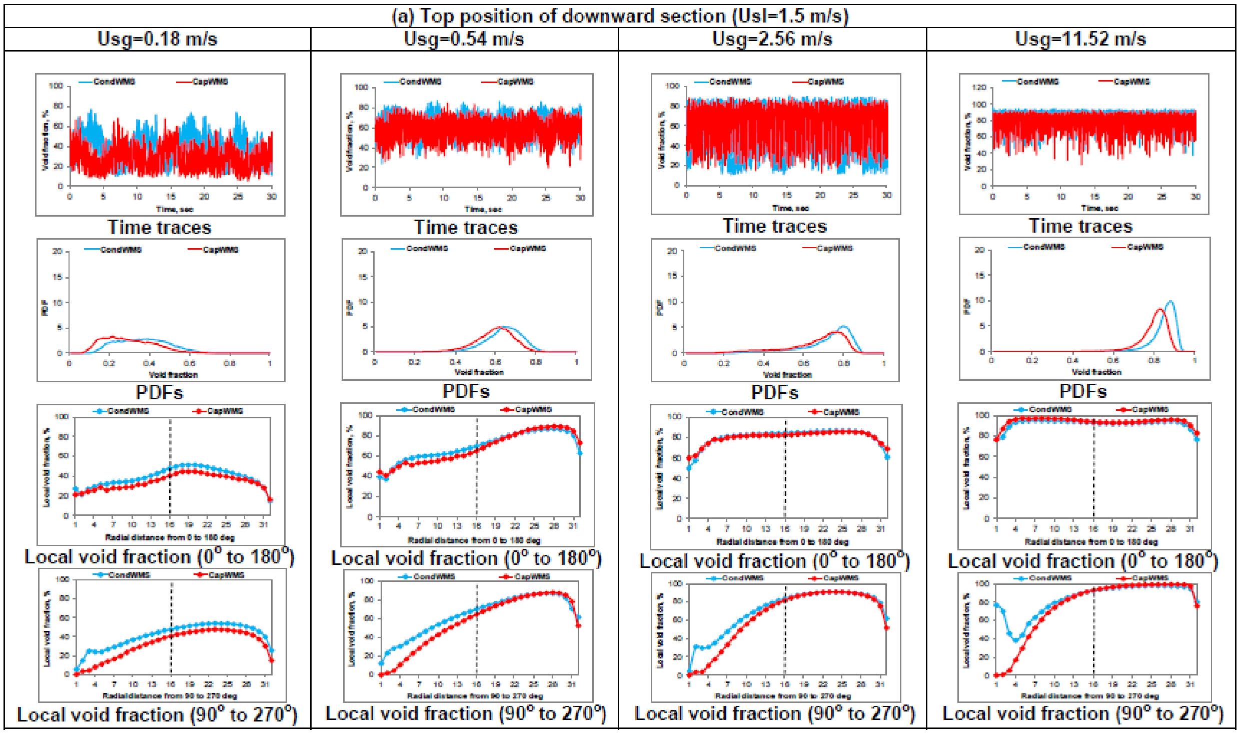

(a)

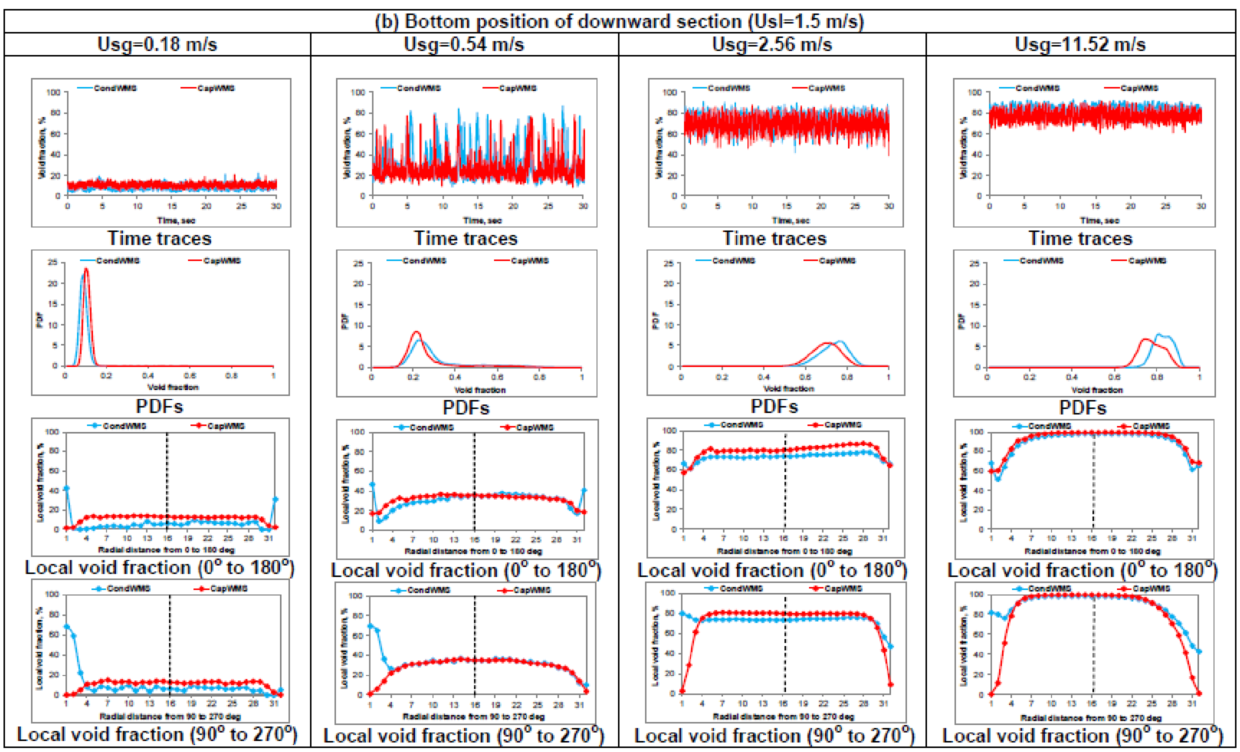

(b)

Figure 5: Distribution of gas void fraction at (a) higher and (b) lower locations of downward orientation

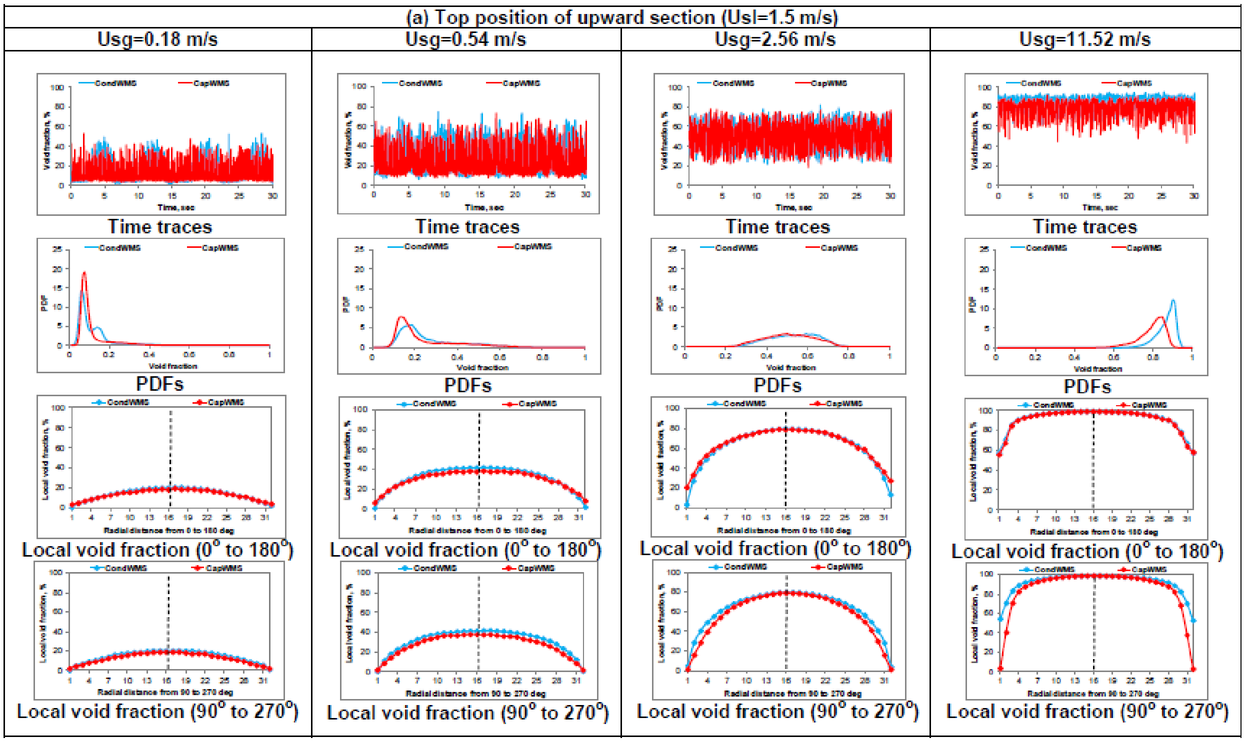

(a)

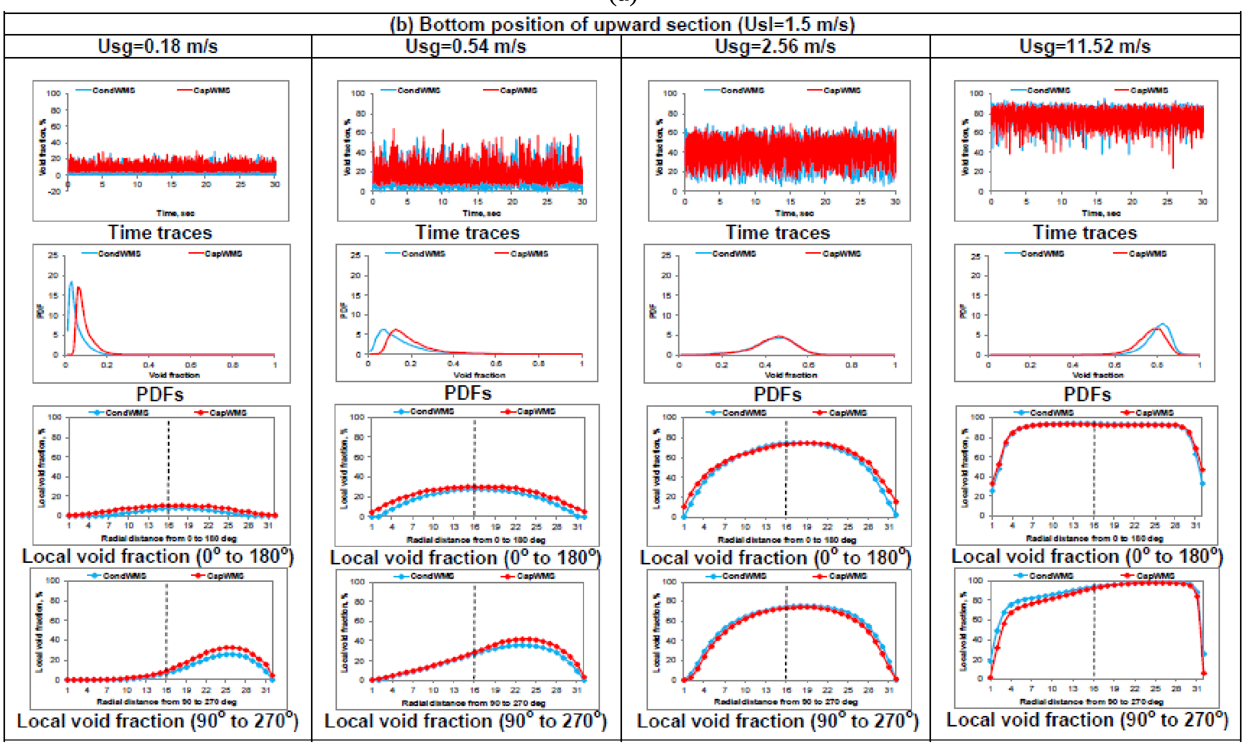

(b)

Figure 6: Distribution of gas void fraction at (a) higher and (b) lower locations of upward orientation

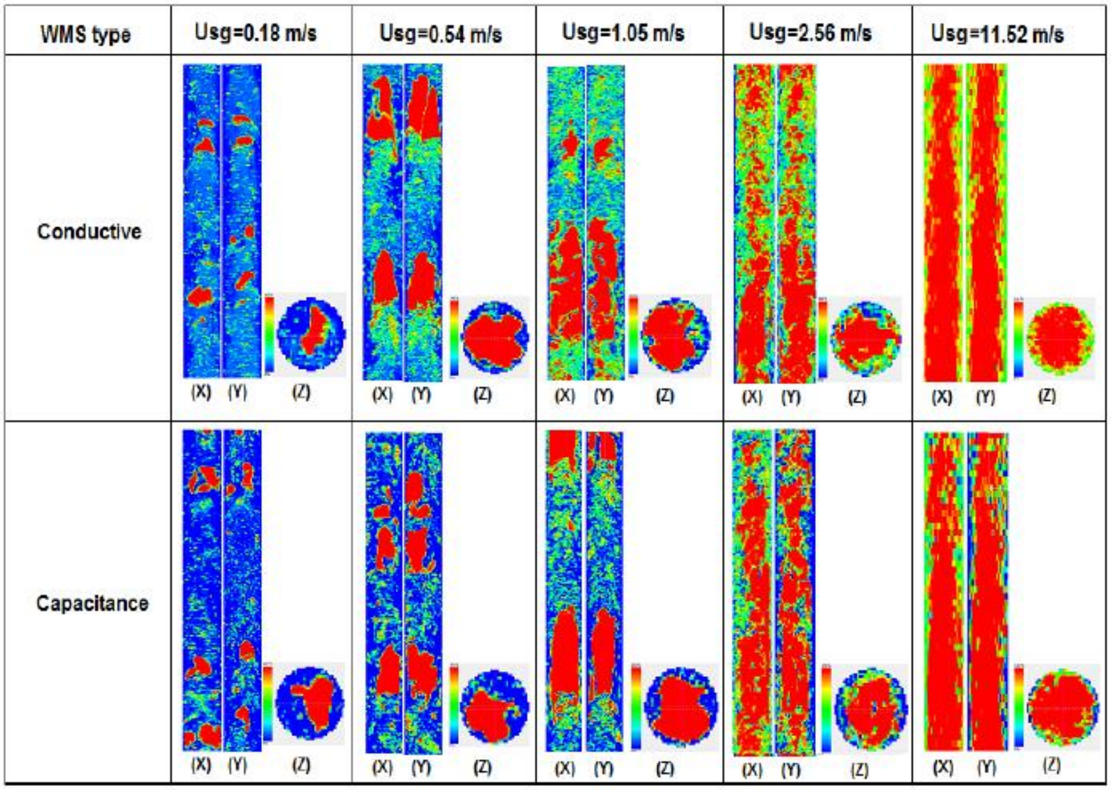

Figure 7: Reconstructed images generated by CondWMS and CapWMS at the higher location of upward orientation (X and Y depict an axially sliced images, and Z depict cross-sectional images)